JVI Journals.ASM.org

Generation of a Recombinant Akabane Virus Expressing Enhanced Green Fluorescent Protein

Akiko Takenaka-Uema,[a,b] Yousuke Murata,[c] Fumihiro Gen,[a,b] Yukari Ishihara-Saeki,[a*] Ken-ichi Watanabe,[c] Kazuyuki Uchida,[c] Kentaro Kato,[a*] Shin Murakami,[a] Takeshi Haga,[b] Hiroomi Akashi,[a] Taisuke Horimoto[a]

Department of Veterinary Microbiology, Graduate School of Agricultural and Life Sciences, The University of Tokyo, Tokyo, Japan[a]; Department of Infection Control and Disease Prevention, Graduate School of Agricultural and Life Sciences, The University of Tokyo, Tokyo, Japan[b]; Department of Veterinary Pathology, Graduate School of Agricultural and Life Sciences, The University of Tokyo, Tokyo, Japan[c]

ABSTRACT

We generated a recombinant Akabane virus (AKAV) expressing enhanced green fluorescence protein (eGFP-AKAV) by using reverse genetics. We artificially constructed an ambisense AKAV S genome encoding N/NSs on the negative-sense strand, and eGFP on the positive-sense strand with an intergenic region (IGR) derived from the Rift Valley fever virus (RVFV) S genome. The recombinant virus exhibited eGFP fluorescence and had a cytopathic effect in cell cultures, even after several passages. These results indicate that the gene encoding eGFP in the ambisense RNA could be stably maintained. Transcription of N/NSs and eGFP mRNAs of eGFP-AKAV was terminated within the IGR. The mechanism responsible for this appears to be different from that in RVFV, where the termination sites for N and NSs are determined by a defined signal sequence. We inoculated suckling mice intraperitoneally with eGFP-AKAV, which resulted in neurological signs and lethality equivalent to those seen for the parent AKAV. Fluorescence from eGFP in frozen brain slices from the eGFP-AKAV-infected mice was localized to the cerebellum, pons, and medulla oblongata. Our approach to producing a fluorescent virus, using an ambisense genome, helped obtain eGFP-AKAV, a fluorescent bunyavirus whose viral genes are intact and which can be easily visualized.

IMPORTANCE

AKAV is the etiological agent of arthrogryposis-hydranencephaly syndrome in ruminants, which causes considerable economic loss to the livestock industry. We successfully generated a recombinant enhanced green fluorescent protein-tagged AKAV containing an artificial ambisense S genome. This virus could become a useful tool for analyzing AKAV pathogenesis in host animals. In addition, our approach of using an ambisense genome to generate an orthobunyavirus stably expressing a foreign gene could contribute to establishing alternative vaccine strategies, such as bivalent vaccine virus constructs, for veterinary use against infectious diseases.

Akabane virus (AKAV) is an *Orthobunyavirus* within the family *Bunyaviridae* and the etiological agent of arthrogryposis-hydranencephaly syndrome in cattle, sheep, and goats. Arthrogryposis-hydranencephaly syndrome is characterized by abortion, stillbirth, premature birth, and congenital deformities and is responsible for considerable economic losses to the cattle industry (1). The virus is transmitted primarily by biting midges of the genus *Culicoides* and is widely distributed throughout Australia, Southeast Asia, East Asia, the Middle East, and Africa. AKAV is genetically related to Schmallenberg virus, a recently isolated orthobunyavirus that causes arthrogryposis-hydranencephaly syndrome in ruminants across large areas of Europe (2).

Bunyaviruses are characterized by a tripartite negative-sense RNA genome with large (L), medium (M), and small (S) segments. The L segment encodes the large protein, which acts as the RNA-dependent RNA polymerase (RdRp) in the ribonucleoprotein complex. The M segment encodes two envelope glycoproteins, Gn and Gc, and the nonstructural protein NSm. The glycoproteins are responsible for attachment to cell receptors, while the function of NSm remains unknown. The Gc protein is a major virus-neutralizing antigen. The S segment encodes a nucleoprotein, N, and a nonstructural protein, NSs. N shares antigenic determinants with some other virus species in the genus. NSs acts as a type I interferon antagonist and contributes to the regulation of host protein synthesis (3). Orthobunyavirus N and NSs proteins are encoded by overlapping open reading frames (ORFs) on a single mRNA (4–7). However, phleboviruses, such as Rift Valley fever virus (RVFV), utilize an ambisense strand strategy to express N and NSs (8). The N ORF is on the negative-sense strand, while the NSs ORF is on the positive-sense strand. These two ORFs are separated by a cytosine-rich intergenic region (IGR) (Fig. 1A).

Our understanding of AKAV pathogenesis in ruminants is limited because studying the virus requires biosafety level 2 biocontainment facilities that can handle large virus-infected animals. As

Received 12 March 2015 **Accepted** 29 June 2015

Accepted manuscript posted online 8 July 2015

Citation Takenaka-Uema A, Murata Y, Gen F, Ishihara-Saeki Y, Watanabe KI, Uchida K, Kato K, Murakami S, Haga T, Akashi H, Horimoto T. 2015. Generation of a recombinant Akabane virus expressing enhanced green fluorescent protein. J Virol 89:9477–9484. doi:10.1128/JVI.00681-15.

Editor: D. S. Lyles

Address correspondence to Taisuke Horimoto, ahorimo@mail.ecc.u-tokyo.ac.jp, or Hiroomi Akashi, akashi@mail.ecc.u-tokyo.ac.jp.

* Present address: Yukari Ishihara-Saeki, CEVA-JAPAN K. K., Yokohama, Japan; Kentaro Kato, National Research Center for Protozoan Diseases, Obihiro University of Agriculture and Veterinary Medicine, Obihiro, Japan.

doi:10.1128/JVI.00681-15

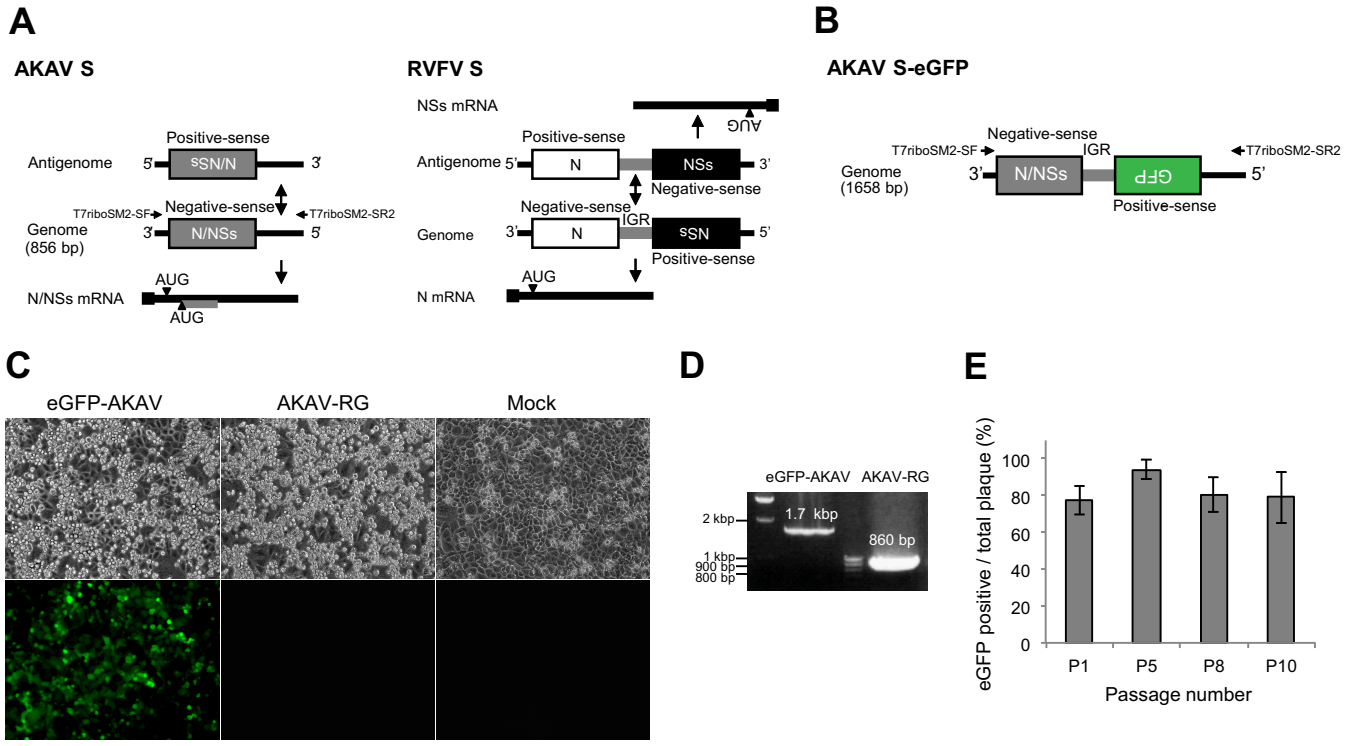

FIG 1 (A) Schematic depiction of negative-sense (AKAV) and ambisense (RVFV) gene expression strategies. AKAV, with a negative-sense strand-coding strategy, possesses an S RNA segment that contains a single transcriptional unit flanked by UTRs. The corresponding positive-sense antigenome is assumed to be transcriptionally silent. The transcriptional unit comprises overlapping ORFs accessed by alternative initiation codons. The gray bar in the N/NSs mRNA represents the NSs ORF region. RVFV, with an ambisense coding strategy, is able to transcribe mRNAs from genomic and antigenomic S RNA strands, with transcription termination signals positioned in a central IGR. A black square indicates a 5′ cap structure on mRNAs. (B) The S-eGFP plasmid was generated using RVFV and an ambisense strategy and was then used to generate eGFP-AKAV. (C) CPE and green fluorescent expression in cells infected with eGFP-AKAV or AKAV-RG or in mock-infected cells. Bright-field (top) and fluorescence (bottom) images are shown. (D) HmLu-1 cells were infected with recombinant or parental virus and analyzed using RT-PCR and electrophoresis to detect S segment RNA. The pair of primers (T7riboSM2-SF and -SR2) used for RT-PCR is indicated in panels A and B. (E) Genetic stability of eGFP-AKAV. HmLu-1 cells were infected with various dilutions of eGFP-AKAV at passages 1, 5, 8, and 10. At 3 days p.i., the number of eGFP-positive plaques was determined. The results are presented as the means ± standard deviations (SD) (error bars) from 4 or 5 wells.

an alternative, rodents are used for the *in vivo* study of AKAV. Mice are often experimentally infected with AKAV via the subcutaneous or intraperitoneal route to assess its pathogenesis (9, 10). Pregnant hamsters can be used as a transplacental-infection model (11), and embryonated chicken eggs can be used as a teratogenic model (12).

Fluorescent viruses are useful in studying viral pathogenesis, as the movement of viral particles can be easily traced and monitored *in vivo*. In a previous study, the orthobunyavirus Bunyamwera virus (BUNV) was used to generate a recombinant virus carrying the enhanced green fluorescent protein (eGFP) fused with a truncated Gc protein (13). The deleted region of the Gc protein was not essential for replication in cell culture (14). However, the inserted eGFP gene was not genetically stable when the virus was subjected to several passages in cell culture.

In the current study, we inserted the eGFP gene and IGR sequence of RVFV downstream of the N/NSs genes in the AKAV S genome using an ambisense strategy to generate an eGFP-tagged AKAV. The resulting recombinant virus, eGFP-AKAV, replicated efficiently in cell culture, stably expressed eGFP, and displayed neurovirulence similar to that of the parental wild-type virus in mice. In addition, we were able to identify viral infection in subregions of the mouse brain easily using fluorescence imaging.

MATERIALS AND METHODS

Cells and viruses. Baby hamster kidney cells stably expressing T7 RNA polymerase (BHK/T7-9 cells) (15) were kindly provided by Naoto Ito (Gifu University, Japan) and cultured at 37°C in Eagle's minimum essential medium (MEM) supplemented with 5% fetal calf serum (FCS) and 10% tryptose phosphate broth. Hamster lung (HmLu-1) cells were cultured at 37°C in Dulbecco's modified Eagle's medium (DMEM) supplemented with 5% FCS. We used the neurovirulent Iriki strain of AKAV (16) in this study to derive a recombinant virus. Viruses were propagated in HmLu-1 cells cultured in serum-free medium.

Plasmid generation. We previously established a T7 RNA polymerase-driven reverse-genetics system for AKAV (A. Takenaka-Uema, K. Sugiura, N. Bangphoomi, C. Shioda, K. Uchida, K. Kato, T. Haga, S. Murakami, H. Akashi, and T. Horimoto, submitted for publication). We generated three plasmids expressing viral RNAs, which were designated pT7riboSM2/IL, pT7riboSM2/IM, and pT7riboSM2/IS, in which cDNAs from the L, M, or S segments, respectively, of the Iriki strain were cloned. The pT7riboSM2/IS plasmid was used to generate pT7riboSM2/S-eGFP, where the eGFP gene was inserted in the opposite orientation to the N gene. The coding region for eGFP was amplified from pEGFP-N1 (Clontech). A 30-bp sequence of the 5′ untranslated region (UTR) from the S segment was added as a flanking sequence upstream of the eGFP ORF by PCR, using primers IrikiS-3′NCR+GFP-F (5′-GAA GCA AGG AAA CTG GAG AAT CAG CAA AGA ATG GTG AGC AAG GGC GAG GAG-

3′) and MluI+GFP-R (5′-AAA ACG CGT TTA CTT GTA CAG CTC GTC CAT-3′). The full-length 5′ UTR (135 bp) of the S segment was amplified using primers IrikiS-3′NCR-F (5′-TCT TTG CTG ATT CTC CAG TT-3′) and T7riboSM2-SR2 (5′-AAT CGT CTC CAC CCA GTA GTG TTC T-3′). These two overlapping fragments, eGFP plus the partial 5′ UTR and the entire 5′ UTR of the S segment, were used as PCR templates, with primers T7riboSM2-SR2 and MluI+GFP-R added to reaction mixtures. The resulting amplified fragment contained the eGFP ORF and the entire 5′ UTR of the S fragment. A 55-bp sequence from the 5′ end of the RVFV strain ZH548 (GenBank accession no. DQ380151) IGR was added downstream of this fragment in a stepwise manner by using primers T7riboSM2-SR2 and GFP+IGR-R1 (5′-GGG GGG TGG GGG GTG GGG CAG CCT TAA CCT TTA CTT GTA CAG CTC GTC CAT-3′) and then primers T7riboSM2-SR2 and GFP+IGR-R2 (5′-GGG AGT TGG GGT TAC GGT CGG GAT TGG GGG GTG GGG GGT GGG GCA G-3′). The 3′ end of the IGR (57 bp) was added downstream of the N/NSs ORF by extension using primers T7riboSM2-SF (5′-AAT CGT CTC CTA TAG AGT AGT GAA CT-3′) and IrikiS+IGR-R (5′-CCC CCA ATC CCG ACC GTA ACC CCA ACT CCC CTT CCC CCC AAC CCC CTG GGC AGC CAC TTA GAT CTG AAT ACC AAA TTG AG-3′). Two IGR-overlapping fragments, the 3′ end of the IGR with the N/NSs ORF and the 5′ end of the IGR with the eGFP ORF, were used as PCR templates with the primers T7robpSM2-SF and T7riboSM2-SR2. This produced an ambisense S segment, designated S-eGFP, which contained the N/NSs gene, IGR sequence, and eGFP gene. We inserted S-eGFP into the pT7riboSM2 vector (17) at the Esp3I restriction site, yielding pT7riboSM2/S-eGFP.

Generation of recombinant viruses. We used pT7riboSM2/IL, pT7riboSM2/IM, and pT7riboSM2/IS for reverse genetics to efficiently produce a recombinant form of wild-type AKAV (AKAV-RG), which we used as a control virus. To generate eGFP-AKAV, subconfluent BHK/T7-9 cells grown in 6-well plates were transfected with 1.2 μg each of pT7riboSM2/IL and pT7riboSM2/S-eGFP and 0.6 μg of pT7riboSM2/IM by using 9 μl of TransIt-LT1 transfection reagent (Mirus) in 200 μl of Opti-MEM (GIBCO). At 3 days posttransfection, the culture supernatants of transfected cells were harvested and added to HmLu-1 cells. Viruses were plaque purified three times from HmLu-1 cells and stored until required. The presence of recombinant virus was confirmed by the appearance of cytopathic effects (CPE) and expression of eGFP, which was monitored using a Nikon Eclipse TS100 fluorescence microscope (Nikon, Japan). Titers of recombinant viruses were determined using plaque assays as previously described (18).

Reverse transcription (RT)-PCR analysis. Viral RNA was extracted from the supernatants of infected cell cultures by using a QIAamp viral RNA minikit (Qiagen) according to the manufacturer's instructions. To synthesize cDNAs, we used SuperScript III reverse transcriptase (Invitrogen) and primers T7riboSM2-SF, T7riboSM2-MF, and T7riboSM2-LF for the 3′ ends of the S, M, and L segments, respectively. The three segments of the recombinant virus were amplified by PCR using LA *Taq* polymerase (TaKaRa Bio). Primers T7riboSM2-SF and T7riboSM2-SR2 were used for the S RNA segment, T7riboSM2-MF (5′-AAT CGT CTC CTA TAG AGT AGT GAA CTA CCA CAA CAA AAT G-3′) and T7riboSM2-MR (5′-AAT CGT CTC CAC CCA GTA GTG TTC TAC CAC AAC AAA TAA TTA T-3′) for the M RNA segment, and T7riboSM2-LF (5′-AAT CGT CTC CTA TAG AGT AGT GTA CCC CTA AAT ACA ACA TAC A-3′) and T7riboSM2-LR (5′-AAT CGT CTC CAC CCA GTA GTG TGC CCC TAA ATG CAA TAA TAT-3′) for the L RNA segment. The resulting amplicons were analyzed by agarose gel electrophoresis, and DNA bands of the correct sizes were recovered and purified using a NucleoSpin Gel and PCR cleanup kit (TaKaRa Bio). The purified DNA products were digested with the appropriate restriction enzyme, and S-eGFP was sequenced using standard protocols and a 3130xl genetic analyzer (Applied Biosystems).

Growth kinetics and plaque morphology. A subconfluent HmLu-1 cell monolayer was infected with eGFP-AKAV or AKAV-RG at a multiplicity of infection (MOI) of 0.01. After 1 h at 37°C, unbound virus was removed, the cells were washed with phosphate-buffered saline (PBS), and serum-free medium was added. At different time points postinfection (p.i.), supernatants were harvested and titrated using plaque assays with HmLu-1 cells. Experiments were performed in triplicate. To examine differences in plaque morphology between eGFP-AKAV and AKAV-RG, HmLu-1 cells were seeded into 6-well plates. We added eGFP-AKAV or AKAV-RG to cells and allowed them to incubate at 37°C for 1 h. Then, we removed the virus suspension and covered the cells with DMEM containing 0.8% (wt/vol) agar and 2% FCS. After 4 days, the cells were stained with neutral red.

Counting green fluorescent protein (GFP)-positive plaques. Plaque-purified eGFP-AKAV was serially passaged 10 times in HmLu-1 cells. The HmLu-1 cells were grown in 4-well Lab-Tek chamber slides (Thermo) and infected with diluted eGFP-AKAV at various passages for 1 h at 37°C. Unbound viruses were removed, and the cells were covered with DMEM containing 0.8% methylcellulose and 2% FCS. At 3 days p.i., methylcellulose-containing media were removed, and the cells were washed with PBS three times. Live cells were observed using a Zeiss LSM 510 confocal microscope. The total number of plaques was determined, and the numbers of fluorescent plaques at different virus passages were compared. Data were collected from at least four wells for each sample of diluted eGFP-AKAV.

Immunofluorescence assays. For immunofluorescence imaging of eGFP-AKAV, subconfluent monolayers of HmLu-1 cells grown in 4-well Lab-Tek chamber slides were infected with eGFP-AKAV at an MOI of 0.01 for 1 h at 37°C. After removal of unbound virus, the cells were overlaid with DMEM containing 0.8% methylcellulose and 2% FCS. At 2 days p.i., methylcellulose-containing media were removed and the cells were washed with PBS. Cells were fixed with 4% paraformaldehyde and permeabilized with 0.3% Triton X-100 in PBS for 5 min. Following washes with PBS and blocking for 30 min, the cells were incubated for 1 h with rabbit antiserum against AKAV (19), followed by incubation with Alexa 546-conjugated anti-rabbit IgGs for 1 h. The cells were washed with PBS and allowed to dry. Samples were mounted in fluorescent mounting medium (Dako) and covered with coverslips. The slides were stored in the dark at 4°C until they were analyzed. Fluorescence images were acquired using a Zeiss LSM 510 confocal microscope.

3′ rapid amplification of cDNA ends (RACE). Total RNA was extracted from infected HmLu-1 cells and polyadenylated *in vitro* using an A-Plus Poly(A) polymerase tailing kit (Epicenter Biotechnologies), according to the manufacturer's instructions. Samples were subsequently purified using a QIAamp viral RNA minikit, following standard protocols. Approximately 1 μg of polyadenylated RNA was used as the template for reverse transcription with an oligo(dT)-containing primer (3′ RACE-AP; Invitrogen). After reverse transcription, cDNAs were subjected to PCR amplification with LA *Taq* polymerase using primers homologous to the adapter region of the amplification primer (AUAP; Invitrogen) and S-0F, a primer specific for AKAV S (5′-CAT TTT CAA CGA TGT TCC AC-3′), or GFP-F1, a primer specific for eGFP (5′-ATG GTG AGC AAG GGC GAG GA-3′). Part of the amplified PCR products was used as the template for seminested amplification. The AUAP primer and either S459-478 (5′-GGG ATT TGC CCC TGG TGC TG-3′) or GFP-363F (5′-GAA CCG CAT CGA GCT GAA GG-3′) were used for the second round of AKAV S or eGFP amplification, respectively. The resulting PCR products were analyzed by agarose gel electrophoresis, and DNA bands of the correct sizes were recovered and purified. The purified DNA products were cloned into pCR2.1-TOPO (Invitrogen) and sequenced.

Animal infection and pathological analysis of brains. We intraperitoneally administered AKAV-RG or GFP-AKAV (5×10^4 PFU or 5×10^5 PFU per 0.1-ml dose) to BALB/cCrSlc mice (3 days old; Japan SLC). The mice were observed for mortality over 21 days. Animals that were moribund during the observation period were sacrificed, and their brains were collected. For fluorescence imaging, the brains were embedded in Tissue-Tek O.C.T Compound (Sakura), frozen in liquid nitrogen, and stored at −80°C until required. Consecutive 12-μm sections were cut coronally

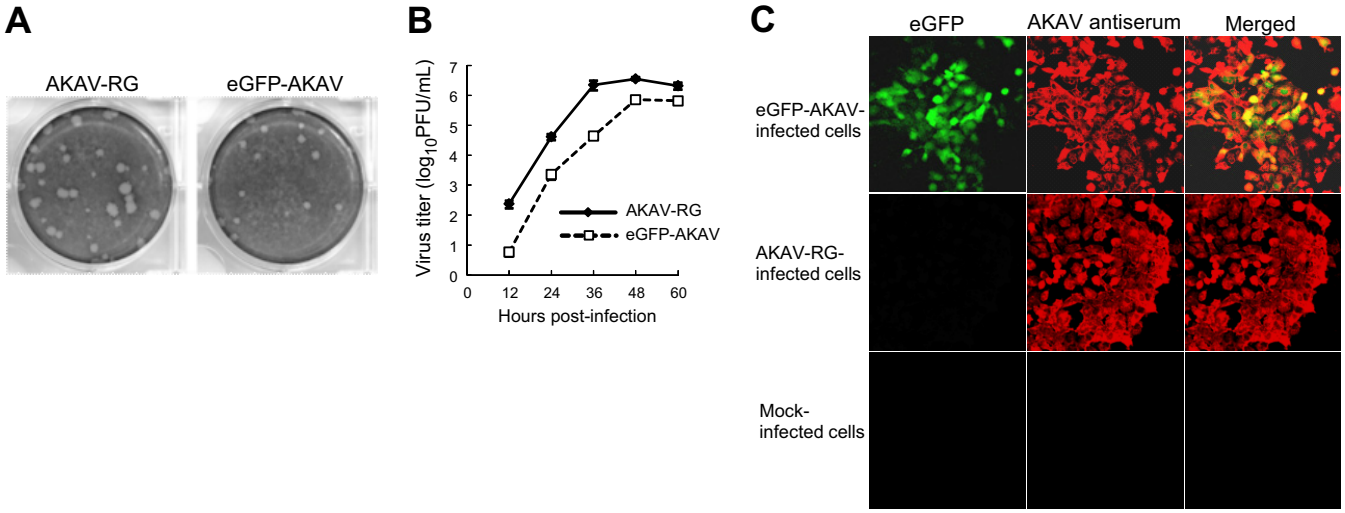

FIG 2 Plaque morphology and growth kinetics of recombinant viruses. (A) Comparison of plaque sizes between AKAV-RG and eGFP-AKAV. (B) Growth curves for AKAV-RG and eGFP-AKAV in HmLu-1 cells. HmLu-1 cells were infected with eGFP-AKAV or AKAV-RG at an MOI of 0.01. The results are presented as the means ± SD (error bars) from three independent experiments. (C) Fluorescence microscopic analysis of cells infected with eGFP-AKAV. HmLu-1 cells were infected with eGFP-AKAV or AKAV-RG at an MOI of 0.01. (Left) eGFP fluorescence in cells infected with eGFP-AKAV or AKAV-RG or in mock-infected cells. (Middle) Infected cells that were incubated with an AKAV antiserum. (Right) Colocalization of AKAV antigens (red) and eGFP fluorescence (green).

with a CM3050 S cryostat (Leica) and placed onto silane-coated glass slides. Sections were mounted in Vectashield mounting medium with DAPI (4′,6-diamidino-2-phenylindole) (Vector Laboratories), covered with coverslips, and stored in the dark at 4°C until required. Images were acquired using a Leica DMI 300B microscope. Animal experiments were conducted with the approval of the University of Tokyo under the guidelines for animal and recombinant DNA experiments. For the detection of AKAV antigen, brains were fixed with 4% phosphate-buffered paraformaldehyde and processed for paraffin embedding. Serial sections mounted on slides were subjected to immunostaining using the Envision polymer method (Dako). Rabbit antiserum against the AKAV OBE-1 strain (20) (1:200 dilution) was used as the primary antibody (19). Immunoreactivity was visualized with 3,3′-diaminobenzidine. Virus titers in the brains of sacrificed mice were determined by a plaque assay with HmLu-1 cells using a 20% homogenate of the organs in the medium.

RESULTS

Generation of eGFP-AKAV. Transcriptional termination of N and NSs mRNAs of phlebovirus, such as RVFV, occurs at an IGR between the N and NSs ORFs (Fig. 1A). Although orthobunyavirus does not use an ambisense strategy to express N and NSs proteins, the BUNV S RNA possesses potential ambisense transcriptional promoters (21). We tested whether the ambisense strategy works in AKAV S RNA by introducing the RVFV IGR into the 3′ flanking region of the N/NSs ORF and the coding sequence of eGFP to generate S-eGFP (Fig. 1B). To produce eGFP-AKAV, we cotransfected S-eGFP, along with the L and M RNA expression plasmids, into BHK/T7-9 cells. At 3 days posttransfection, the supernatants of transfected cells were collected and used to infect fresh HmLu-1 cells. At 2 days p.i., we observed eGFP signals and CPE in HmLu-1 cell cultures (Fig. 1C). To examine whether eGFP-AKAV maintained the full-length S-eGFP RNA, we used RT-PCR assays to confirm the presence of a 1.7-kb product, indicative of S-eGFP (Fig. 1D). We confirmed that the nucleotide sequence of S RNA in eGFP-AKAV did not possess any unwanted mutations or deletions. To evaluate the genetic stability of eGFP-AKAV, it was serially passaged 10 times in HmLu-1 cells. The number of eGFP-positive plaques at each passage was determined, and ratios of eGFP-positive plaques to eGFP-AKAV plaques were calculated. A decrease in these ratios was not observed (Fig. 1E). Interestingly, some of the small eGFP-negative plaques were observed to show fluorescence at later observation points when the plaques became larger, suggesting delayed appearance of eGFP signals. This observation was supported by sequence analysis of viruses from eGFP-negative plaques, which showed that the eGFP gene in the S segment had no mutation. Our data demonstrate that we successfully generated a genetically stable eGFP-expressing ambisense AKAV.

Characterization of eGFP-AKAV *in vitro*. To examine the effects of inserting the IGR and eGFP into the S RNA on eGFP-AKAV growth in cell culture, we determined plaque phenotypes and growth kinetics in HmLu-1 cells. Recombinant eGFP-AKAV formed plaques significantly smaller than those of the control AKAV-RG (Fig. 2A). In accordance with their plaque sizes, the titers for eGFP-AKAV were 5-fold lower than those for AKAV-RG. The maximum titers of AKAV-RG and eGFP-AKAV were 3.6×10^6 PFU/ml and 7.2×10^5 PFU/ml, respectively, at 48 h postinfection (Fig. 2B). To test whether eGFP-AKAV-infected cells expressed eGFP, we incubated infected cells with an antibody against AKAV at 2 days p.i. An eGFP signal was absent in cells infected with the control AKAV-RG (Fig. 2C). Although AKAV proteins were detected in eGFP-negative cells, eGFP signals were detected only in eGFP-AKAV-infected cells (Fig. 2C), suggesting low levels of eGFP expression in infected cells. Notably, CPE was followed by the appearance of green fluorescence, indicating delayed expression of eGFP in the infected cells. This could explain the higher intensity of signals from AKAV proteins than those for eGFP in eGFP-AKAV-infected cells (Fig. 2C).

Transcriptional termination of eGFP-AKAV N/NSs and eGFP mRNAs. Termination of RVFV S segment mRNA transcription occurs at a defined termination signal (3′-CGUCG-5′) in the IGR (22, 23). However, for S-eGFP in eGFP-AKAV,

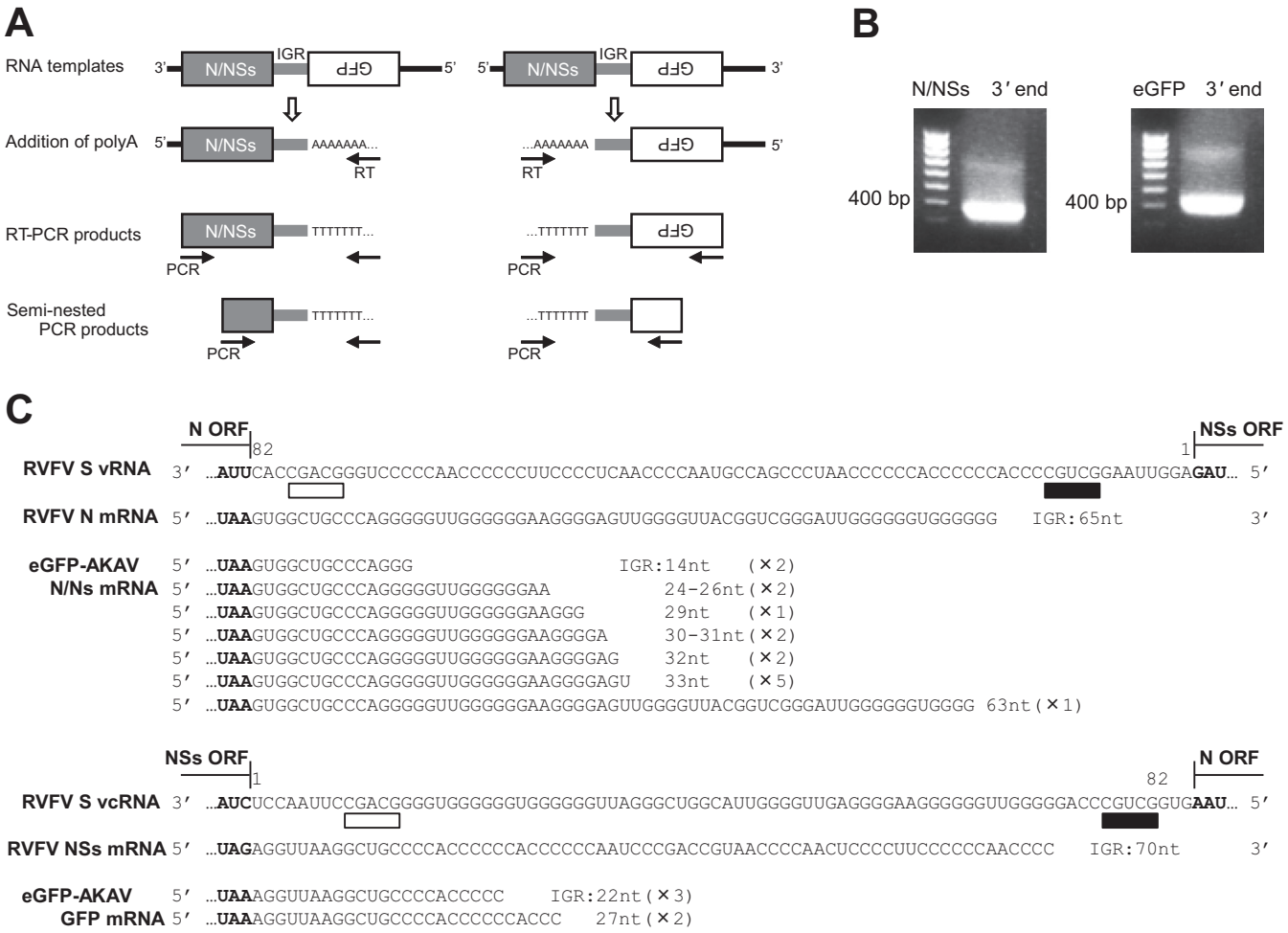

FIG 3 Analysis of mRNAs transcribed from S-eGFP using 3′ RACE. (A) Schematic of the 3′ RACE strategy employed to detect sense and antisense strands of S RNA and mRNA species of N/NSs and eGFP. (B) 3′ RACE amplification of eGFP-AKAV N/NSs and eGFP mRNAs. (C) Mapping of the 3′ location of eGFP-AKAV N/NSs and eGFP. Sequences of viral RNA (vRNA) or viral cRNA (vcRNA) templates, RVFV N or NSs mRNA sequences, and eGFP-AKAV N/NSs or eGFP mRNA sequences are aligned. Boldface indicates the positions of stop codons for RVFV N and NSs or eGFP-AKAV N/NSs and eGFP. The IGR of RVFV strain ZH548 is at positions 1 to 82. The transcriptional termination signal (3′-CGUCG-5′) of RVFV is underlined in black, with RVFV N and NSs mRNA species terminating 4 nt prior to the motif. The 3′-CGACG-5′ motif (underlined in white) represents the transcriptional termination signal for the corresponding ambisense ORF. The 3′ ends of eGFP-AKAV were determined by sequencing cloned 3′ RACE products. The numbers in parentheses indicate how often an identical sequence was identified.

whether this signal is functional for transcriptional termination is unknown. We determined a transcriptional termination site in S-eGFP using 3′ RACE (Fig. 3A). Using a seminested PCR approach, we obtained 3′-terminal amplification products corresponding to the N/NSs (~360-bp) and eGFP (~430-bp) mRNAs (Fig. 3B). Sequencing analysis of these products indicated the presence of several transcriptional termination sites (Fig. 3C). Most of the transcriptional termination sites in N/NSs and eGFP mRNAs were located further upstream than those for RVFV N and NSs mRNAs. The eGFP-AKAV N/NSs mRNA ends were located around nucleotides (nt) 14 to 33 of the IGR in 14 of 15 clones, with one clone in which it was at nucleotide 63. The RVFV N mRNA ends are at nucleotide 65 of the IGR. For RVFV NSs mRNAs, the ends are located at nucleotide 70 of the IGR. The eGFP-AKAV eGFP mRNA ends were located at nucleotide 22 (3 clones) or 27 (2 clones) of the IGR (Fig. 3C). These data suggest that N/NSs and GFP mRNAs of S-eGFP use transcriptional termination mechanisms different from those in RVFV.

Characterization of eGFP-AKAV *in vivo*. To assess the pathogenesis of eGFP-AKAV or AKAV-RG in animals, mice were experimentally infected with 5×10^4 PFU of these viruses. The majority of mice infected with eGFP-AKAV or AKAV-RG exhibited clinical signs of infection, which became apparent at 4 to 13 days p.i. There was no discernible difference in disease progression between the two groups. Approximately half of the mice infected with eGFP-AKAV or AKAV-RG exhibited neurological symptoms, such as hind limb paralysis, and subsequently died; the mortality rate was 50 to 60% (Fig. 4A). Surviving mice also presented with hind limb convulsion, diarrhea, ruffled fur, and a conjunctivitis-like inflammatory response.

We also measured virus titers in the brains of the moribund mice infected with 5×10^5 PFU of eGFP-AKAV or AKAV-RG. There was no significant difference in the titers for the samples from the two groups of virus-infected mice (3 each) (8.0×10^7, 6.3×10^7, and 4.3×10^6 PFU/g for eGFP-AKAV-infected mice versus 2.8×10^8, 9.3×10^5, and 2.5×10^5 PFU/g for AKAV-RG-

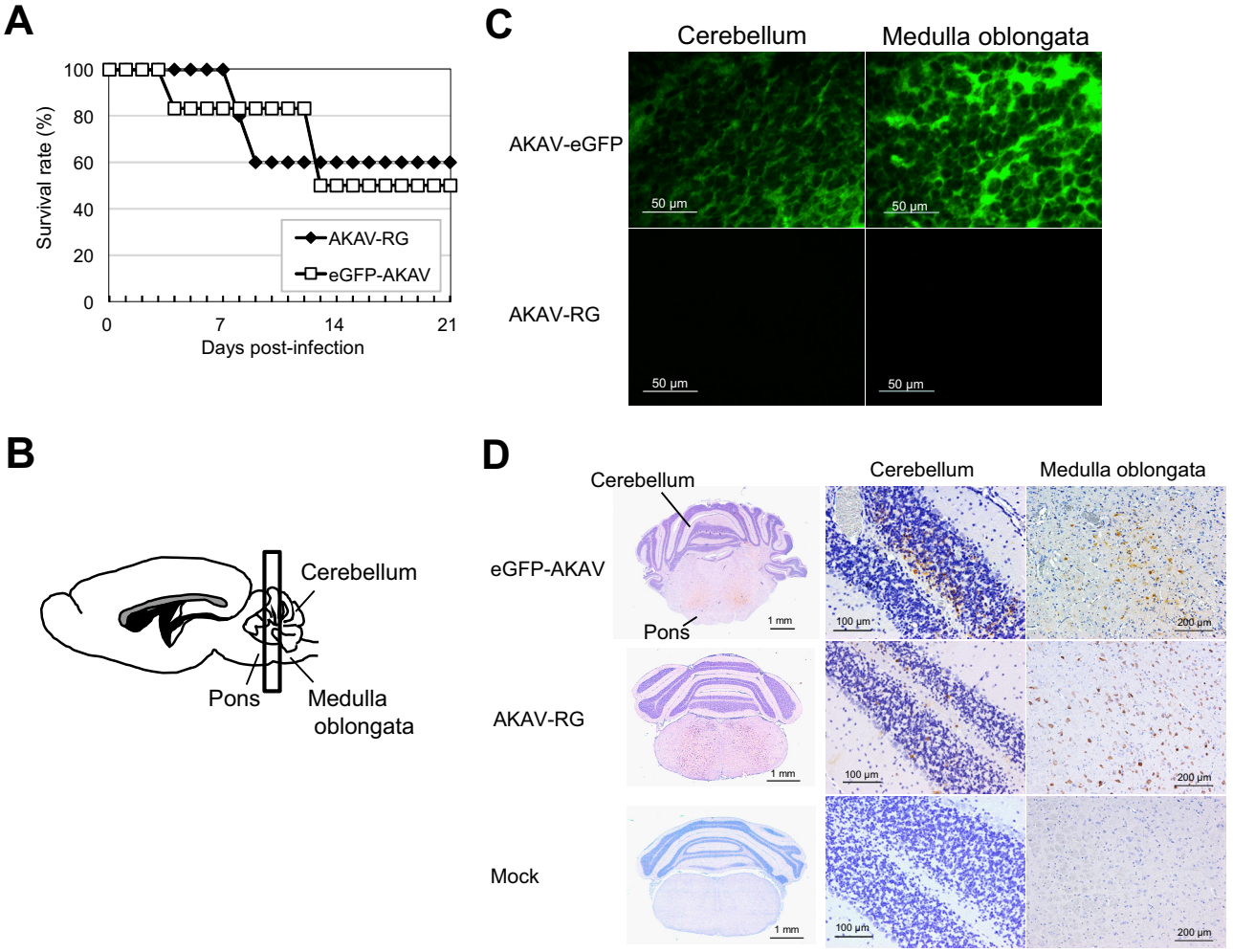

FIG 4 Experimental infection of mice with recombinant AKAVs. Mice were intraperitoneally infected with eGFP-AKAV or AKAV-RG and monitored for 21 days. (A) Survival curves of mice after injection with 5×10^4 PFU of virus. (B) Localization of virus in coronal brain sections. (C) Distribution of eGFP fluorescence in frozen brain sections. (D) Paraffin sections of brain tissue from eGFP-AKAV-, AKAV-RG-, and mock-infected mice immunostained for AKAV antigens. Lower (left)- and higher (right)-magnification images demonstrate localization of the virus as shown in panel C. Virus antigens were detected by immunostaining with AKAV antibody.

infected mice). These data demonstrate that, in mice, eGFP-AKAV possesses replication properties and virulence similar to those of AKAV-RG.

To visualize eGFP signals at the lesion sites of mice infected with eGFP-AKAV, moribund mice were euthanized and their brains were collected. Microscopic examination revealed eGFP-expressing foci in the cerebellum and brain stem throughout the pons and medulla oblongata (Fig. 4C). Immunostaining also revealed the presence of AKAV antigens in the cerebellum, pons, and medulla oblongata of eGFP-AKAV-infected mice, similar to that in AKAV-RG-infected mice (Fig. 4D).

DISCUSSION

We successfully generated a recombinant AKAV, which we designated eGFP-AKAV, that stably expressed eGFP. Although eGFP-AKAV was somewhat attenuated in cell culture, it exhibited pathogenicity similar to that of wild-type AKAV in mice, with eGFP expressed in infected tissues.

To generate eGFP-AKAV, we applied an artificial ambisense coding strategy to an orthobunyavirus with a modified S segment, with the eGFP gene inserted into the strand with the opposite sense to that in which the N/NSs gene was located. Although Barr et al. (21) designed an ambisense BUNV that transcribed S mRNA from the negative strand and GFP mRNA from the positive strand, they did not generate a recombinant infectious virus. In this earlier study, GFP was expressed in transfected cells, indicating that the GFP gene in the artificial S segment was transcribed, although the segment was not packaged into BUNV particles. During the course of preparation of our manuscript, van Knippenberg and Elliott successfully generated a recombinant BUNV with an ambisense S RNA segment (24). They used a sensible strategy with mutated 5′- and 3′-terminal nucleotide sequences and altered promoter activity for this ambisense S segment. The recombinant BUNV with NSs deleted that they created expressed GFP. GFP expression in infected cells was detected but decreased throughout passages, unlike our eGFP-AKAV, whose eGFP expression was stably maintained even at 10 passages. We used a different strategy in which our construct with an ambisense AKAV

S genome contained a sequence encoding an IGR derived from the RVFV S segment between the N/NSs and eGFP genes and intact terminal sequences. This resulted in the packaging of the artificial S segment of eGFP-AKAV into viral particles, and the inserted eGFP gene was stably retained after serial passages. Therefore, the eGFP-AKAV generated here is the second functional fluorescent orthobunyavirus generated using an ambisense coding strategy. The stability of the inserted foreign gene highlights the technical superiority of this ambisense strategy for AKAV and could facilitate the generation of other recombinant AKAVs expressing additional proteins. As an example, a bivalent AKAV vaccine expressing a protective antigen from other pathogens could be constructed using the TS-C2 vaccine strain (25) and this unique ambisense strategy.

The UTRs from each segment of the bunyavirus genome direct the RdRp to perform two distinct RNA synthesis activities, genome transcription and replication. For the orthobunyavirus S segment, negative-sense viral RNA acts as the template for transcription and the first step of replication, while the antisense RNA serves only as the template for the second step of replication (21, 26). Unlike orthobunyaviruses, the S segments of viruses in other *Bunyaviridae* genera, such as phlebovirus and tospovirus, perform ambisense transcription, with the genome and antigenome transcriptionally active. Both ends of the UTRs of bunyavirus genome segments have partial complementary sequences with a panhandle structure, suggesting that the double-stranded region formed by the two ends might function as a transcriptional promoter. In this study, a cytoplasmic eGFP signal was observed after CPE was apparent in eGFP-AKAV-infected cells. This could be due to weak transcriptional promoter activity of the antigenomic promoter in the AKAV S RNA. Introducing mutations into the 3′ and 5′ UTRs to make them complementary sequences, as van Knippenberg and Elliott did for generation of the recombinant BUNV containing an ambisense S segment (24), could be effective in enhancing promoter activity for transcription. Previous reports have shown that these types of mutations have conferred robust transcriptional promoter activity in the BUNV S segment (21, 27).

Recently, signals for mRNA transcriptional termination have been identified in some bunyavirus genomes. In BUNV, the S genome contains two transcriptional termination signals within the 5′ UTRs; they share a pentanucleotide motif (3′-UGUCG-5′) (28), although only the upstream signal mediates transcriptional termination in the context of virus infection (29). This pentanucleotide motif is conserved in the sequences of several other orthobunyaviruses from the serogroups California (Lumboo virus) and Bunyamwera (Maguari virus, Northway virus, Batai virus, and Cache Valley virus) (28). For orthobunyaviruses, such as the Inkoo, La Crosse, Germiston, and Snowshoe hare viruses, a conserved motif exhibiting a single nucleotide deviation (3′-CGUCG-5′) could be the transcriptional termination signal. The AKAV S segment also has the CGUCG pentanucleotide motif within the 5′ UTR, although whether it is a termination signal remains to be determined. In RVFV, transcriptional termination occurs at a 3′-CGUCG-5′ motif present in the IGR (22, 23, 30). The 3′ end of the RVFV N mRNA is located 4 nt upstream of the 3′-CGUCG-5′ sequence, which is at nt 9 to 13 in the IGR of the genome template. The RVFV NSs mRNA terminates at position 70, again 4 nt upstream of the 3′-CGUCG-5′ motif in the antigenome template. For the ambisense AKAV S genome, transcriptional termination of N/NSs and eGFP mRNAs occurs at locations different than those for RVFV N and NSs mRNAs, suggesting different transcriptional termination mechanisms for intact and artificial ambisense segments despite possessing identical IGR sequences. This instability in transcriptional termination possibly reduces eGFP gene expression levels, thereby resulting in the delayed appearance of a cytoplasmic fluorescence signal in eGFP-AKAV-infected cells.

The eGFP-AKAV we generated was pathogenic in mice. Mortality rates were similar to those seen for AKAV-RG. Although eGFP-AKAV generated smaller plaques, and maximum virus titers were 5-fold lower than those for AKAV-RG, insertion of a foreign gene did not dramatically affect the virus phenotype. Because of the ambisense strategy we employed, viral genes were retained in their intact forms in the recombinant virus, although this strategy does not guarantee the same expression levels of viral proteins as those of the parent virus. In previous studies involving the generation of recombinant RVFVs expressing foreign genes, such as luciferase (31, 32) or eGFP (31, 33) genes, viral pathogenicity was markedly attenuated in a rat model, possibly due to lack of NSs (33). Fluorescence corresponding to eGFP expression was detected in the brain slices of mice experimentally infected with eGFP-AKAV. The fluorescent foci were consistent with virus replication sites as identified by immunostaining. The eGFP signals were mainly localized to the cerebellum and brain stem in infected mice, which were also target regions for AKAV-RG. This distribution of AKAV antigens is similar to that observed when mice were intraperitoneally infected with the wild-type Iriki strain of AKAV; viral antigens were detected in the cerebrum, cerebellum, and brain stem (34).

In conclusion, a pathogenic phenotype of eGFP-AKAV will allow us to visualize and trace the movement of the virus in infected animals, facilitating further studies that could better elucidate the AKAV life cycle with respect to neurovirulence, transmission, and invasion of the central nervous system.

ACKNOWLEDGMENTS

This study was supported in part by a Research and Development Project for Application in Promoting New Policies in Agriculture, Forestry and Fisheries grant from the Ministry of Agriculture, Forestry and Fisheries and a Grant-in-Aid from the Ministry of Education, Culture, Sports, Science and Technology of Japan.

We are grateful to N. Ito of Gifu University (Gifu, Japan) for providing BHK/T7-9 cells and F. Weber in the Department of Virology at the University of Freiburg (Freiburg, Germany) for providing pT7riboSM2.

REFERENCES

1. **Inaba Y, Matumoto M.** 1990. Akabane virus, p 467–480. *In* Dinter Z, Morein B (ed), Virus infections of ruminants, vol 3. Elsevier Science Publishers, Amsterdam, The Netherlands.
2. **Hoffmann B, Scheuch M, Höper D, Jungblut R, Holsteg M, Schirrmeier H, Eschbaumer M, Goller KV, Wernike K, Fischer M, Breithaupt A, Mettenleiter TC, Beer M.** 2012. Novel orthobunyavirus in cattle, Europe, 2011. Emerg Infect Dis **18:**469–472. http://dx.doi.org/10.3201/eid1803.111905.
3. **Weber F, Bridgen A, Fazakerley JK, Streitenfeld H, Kessler N, Randall RE, Elliott RM.** 2002. Bunyamwera bunyavirus nonstructural protein NSs counteracts the induction of alpha/beta interferon. J Virol **76:**7949–7955. http://dx.doi.org/10.1128/JVI.76.16.7949-7955.2002.
4. **Akashi H, Kaku Y, Kong XG, Pang H.** 1997. Sequence determination and phylogenetic analysis of the Akabane bunyavirus S RNA genome segment. J Gen Virol **78:**2847–2851.
5. **Elliott RM.** 1989. Nucleotide sequence analysis of the small (S) RNA segment of Bunyamwera virus, the prototype of the family Bunyaviridae.

J Gen Virol **70:**1281–1285. http://dx.doi.org/10.1099/0022-1317-70-5-1281.

6. **Fuller F, Bhown AS, Bishop DH.** 1983. Bunyavirus nucleoprotein, N, and a non-structural protein, NSS, are coded by overlapping reading frames in the S RNA. J Gen Virol **64:**1705–1714. http://dx.doi.org/10.1099/0022-1317-64-8-1705.
7. **Fuller F, Bishop DH.** 1982. Identification of virus-coded nonstructural polypeptides in bunyavirus-infected cells. J Virol **41:**643–648.
8. **Giorgi C, Accardi L, Nicoletti L, Gro MC, Takehara K, Hilditch C, Morikawa S, Bishop DH.** 1991. Sequences and coding strategies of the S RNAs of Toscana and Rift Valley fever viruses compared to those of Punta Toro, Sicilian Sandfly fever, and Uukuniemi viruses. Virology **180:**738–753. http://dx.doi.org/10.1016/0042-6822(91)90087-R.
9. **Ogawa Y, Fukutomi T, Sugiura K, Kato K, Tohya Y, Akashi H.** 2007. Comparison of Akabane virus isolated from sentinel cattle in Japan. Vet Microbiol **124:**16–24. http://dx.doi.org/10.1016/j.vetmic.2007.03.020.
10. **Kurogi H, Inaba Y, Takahashi E, Sato K, Akashi H, Satoda K, Omori T.** 1978. Pathogenicity of different strains of Akabane virus for mice. Natl Inst Anim Health Q (Tokyo) **18:**1–7.
11. **Andersen AA, Campbell CH.** 1978. Experimental placental transfer of Akabane virus in the hamster. Am J Vet Res **39:**301–304.
12. **McPhee DA, Parsonson IM, Della-Porta AJ, Jarrett RG.** 1984. Teratogenicity of Australian Simbu serogroup and some other Bunyaviridae viruses: the embryonated chicken egg as a model. Infect Immun **43:**413–420.
13. **Shi X, van Mierlo JT, French A, Elliott RM.** 2010. Visualizing the replication cycle of bunyamwera orthobunyavirus expressing fluorescent protein-tagged Gc glycoprotein. J Virol **84:**8460–8469. http://dx.doi.org/10.1128/JVI.00902-10.
14. **Shi X, Goli J, Clark G, Brauburger K, Elliott RM.** 2009. Functional analysis of the Bunyamwera orthobunyavirus Gc glycoprotein. J Gen Virol **90:**2483–2492. http://dx.doi.org/10.1099/vir.0.013540-0.
15. **Ito N, Takayama-Ito M, Yamada K, Hosokawa J, Sugiyama M, Minamoto N.** 2003. Improved recovery of rabies virus from cloned cDNA using a vaccinia virus-free reverse genetics system. Microbiol Immunol **47:**613–617. http://dx.doi.org/10.1111/j.1348-0421.2003.tb03424.x.
16. **Miyazato S, Miura Y, Hase M, Kubo M, Goto Y, Kono Y.** 1989. Encephalitis of cattle caused by Iriki isolate, a new strain belonging to Akabane virus. Jpn J Vet Sci **51:**128–136. http://dx.doi.org/10.1292/jvms1939.51.128.
17. **Habjan M, Penski N, Spiegel M, Weber F.** 2008. T7 RNA polymerase-dependent and -independent systems for cDNA-based rescue of Rift Valley fever virus. J Gen Virol **89:**2157–2166. http://dx.doi.org/10.1099/vir.0.2008/002097-0.
18. **Ogawa Y, Sugiura K, Kato K, Tohya Y, Akashi H.** 2007. Rescue of Akabane virus (family Bunyaviridae) entirely from cloned cDNAs by using RNA polymerase I. J Gen Virol **88:**3385–3390. http://dx.doi.org/10.1099/vir.0.83173-0.
19. **Tsuda T, Yoshida K, Yanase T, Ohashi S, Yamakawa M.** 2004. Competitive enzyme-linked immunosorbent assay for the detection of the antibodies specific to Akabane virus. J Vet Diagn Invest **16:**571–576. http://dx.doi.org/10.1177/104063870401600613.
20. **Kurogi H, Inaba Y, Takahashi E, Sato K, Omori T, Miura Y, Goto Y, Fujiwara Y, Hatano Y, Kodama K, Fukuyama S, Sasaki N, Matumoto M.** 1976. Epizootic congenital arthrogryposis-hydranencephaly syndrome in cattle: isolation of Akabane virus from affected fetuses. Arch Virol **51:**67–74. http://dx.doi.org/10.1007/BF01317835.
21. **Barr JN, Rodgers JW, Wertz GW.** 2005. The Bunyamwera virus mRNA transcription signal resides within both the 3′ and the 5′ terminal regions and allows ambisense transcription from a model RNA segment. J Virol **79:**12602–12607. http://dx.doi.org/10.1128/JVI.79.19.12602-12607.2005.
22. **Albariño CG, Bird BH, Nichol ST.** 2007. A shared transcription termination signal on negative and ambisense RNA genome segments of Rift Valley fever, sandfly fever Sicilian, and Toscana viruses. J Virol **81:**5246–5256. http://dx.doi.org/10.1128/JVI.02778-06.
23. **Ikegami T, Won S, Peters CJ, Makino S.** 2007. Characterization of Rift Valley fever virus transcriptional terminations. J Virol **81:**8421–8438. http://dx.doi.org/10.1128/JVI.02641-06.
24. **van Knippenberg I, Elliott RM.** 2015. Flexibility of bunyavirus genomes: creation of an orthobunyavirus with an ambisense S segment. J Virol **89:**5525–5535. http://dx.doi.org/10.1128/JVI.03595-14.
25. **Kurogi H, Inaba Y, Takahashi E, Sato K, Akashi H, Satoda K, Omori T.** 1979. An attenuated strain of Akabane virus: a candidate for live virus vaccine. Natl Inst Anim Health Q (Tokyo) **19:**12–22.
26. **Jin H, Elliott RM.** 1993. Characterization of Bunyamwera virus S RNA that is transcribed and replicated by the L protein expressed from recombinant vaccinia virus. J Virol **67:**1396–1404.
27. **Barr JN, Wertz GW.** 2005. Role of the conserved nucleotide mismatch within 3′- and 5′-terminal regions of Bunyamwera virus in signaling transcription. J Virol **79:**3586–3594. http://dx.doi.org/10.1128/JVI.79.6.3586-3594.2005.
28. **Barr JN, Rodgers JW, Wertz GW.** 2006. Identification of the Bunyamwera bunyavirus transcription termination signal. J Gen Virol **87:**189–198. http://dx.doi.org/10.1099/vir.0.81355-0.
29. **Blakqori G, Lowen AC, Elliott RM.** 2012. The small genome segment of Bunyamwera orthobunyavirus harbours a single transcription-termination signal. J Gen Virol **93:**1449–1455. http://dx.doi.org/10.1099/vir.0.042390-0.
30. **Lara E, Billecocq A, Leger P, Bouloy M.** 2011. Characterization of wild-type and alternate transcription termination signals in the Rift Valley fever virus genome. J Virol **85:**12134–12145. http://dx.doi.org/10.1128/JVI.05322-11.
31. **Billecocq A, Gauliard N, Le May N, Elliott RM, Flick R, Bouloy M.** 2008. RNA polymerase I-mediated expression of viral RNA for the rescue of infectious virulent and avirulent Rift Valley fever viruses. Virology **378:**377–384. http://dx.doi.org/10.1016/j.virol.2008.05.033.
32. **Ikegami T, Won S, Peters CJ, Makino S.** 2006. Rescue of infectious Rift Valley fever virus entirely from cDNA, analysis of virus lacking the NSs gene, and expression of a foreign gene. J Virol **80:**2933–2940. http://dx.doi.org/10.1128/JVI.80.6.2933-2940.2006.
33. **Bird BH, Albariño CG, Hartman AL, Erickson BR, Ksiazek TG, Nichol ST.** 2008. Rift Valley fever virus lacking the NSs and NSm genes is highly attenuated, confers protective immunity from virulent virus challenge, and allows for differential identification of infected and vaccinated animals. J Virol **82:**2681–2691. http://dx.doi.org/10.1128/JVI.02501-07.
34. **Murata Y, Uchida K, Shioda C, Uema A, Bangphoomi N, Chambers JK, Akashi H, Nakayama H.** Histopathological studies on the neuropathogenicity of the Iriki and OBE-1 strains of Akabane virus in BALB/cAJcl mice. J Comp Pathol, in press. http://dx.doi.org/10.1016/j.jcpa.2015.06.003.